

No evidence for a volcanic trigger for late Cambrian carbon cycle perturbations

Tracking no: G51570R

Authors:

Joost Frieling (University of Oxford), Tamsin Mather (University of Oxford), Isabel Fendley, Hugh Jenkyns (University of Oxford), Zhengfu Zhao, Tais Dahl (University of Copenhagen), Bridget Bergquist (University of Toronto), Kathryn Cheng (University of Toronto), Arne Nielsen (University of Copenhagen), and Alex Dickson (Royal Holloway University of London)

Abstract:

The Early Paleozoic was marked by several carbon-cycle perturbations and associated carbon-isotope excursions (CIEs). Whether these CIEs are connected to significant (external) triggers, as is often considered to be the case for CIEs in the Mesozoic and Cenozoic, or result from small carbon-cycle imbalances that became amplified through lack of efficient silicate weathering or other feedbacks, remains unclear. We present concentration and isotope data for sedimentary mercury and osmium to assess the impact of subaerial and submarine volcanism and weathering during the late Cambrian and early Ordovician. Data from the Alum Shale Formation (Sweden) cover the Steptoean Positive Carbon Isotope Excursion (SPICE; ca. 497 - 494 million years ago), a period marked by marine anoxia and biotic overturning, and several smaller CIEs extending into the early Ordovician. Our Hg and Os data offer no strong evidence that the CIEs present in our record could have been driven by (globally) elevated volcanism or continental weathering. Organic-carbon and Hg concentrations covary cyclically, providing further evidence of an unperturbed Hg cycle. Mesozoic and Cenozoic CIEs are often linked to enhanced volcanic activity and weathering but similar late Cambrian-Early Ordovician events cannot easily be connected to such external triggers. Our results are more consistent with reduced Early Paleozoic carbon-cycle resilience that allowed small imbalances to develop into large CIEs.

No evidence for a volcanic trigger for late Cambrian carbon cycle perturbations

J. Frieling^{1*}, T.A. Mather¹, I.M. Fendley¹, H.C. Jenkyns¹, Z. Zhao^{2,3}, T.W. Dahl³, B.A. Bergquist⁴, K. Cheng⁴, A.T. Nielsen³, A.J. Dickson⁵

1. Department of Earth Sciences, University of Oxford, UK

2. School of Earth and Space Sciences, Peking University, Beijing, China

3. Department of Geosciences and Natural Resource Management, University of Copenhagen, Denmark

4. Department of Earth Sciences, University of Toronto, Canada

5. Department of Earth Sciences, Royal Holloway University of London, UK

** joost.frieling@earth.ox.ac.uk*

ABSTRACT

The Early Paleozoic was marked by several carbon-cycle perturbations and associated carbon-isotope excursions (CIEs). Whether these CIEs are connected to significant (external) triggers, as is often considered to be the case for CIEs in the Mesozoic and Cenozoic, or result from small carbon-cycle imbalances that became amplified through lack of efficient silicate weathering or other feedbacks, remains unclear. We present concentration and isotope data for sedimentary mercury and osmium to assess the impact of subaerial and submarine volcanism and weathering during the late Cambrian and early Ordovician. Data from the Alum Shale Formation (Sweden) cover the Steptoean Positive Carbon Isotope Excursion (SPICE; *ca.* 497 – 494 million years ago), a period marked by marine anoxia and biotic overturning, and several smaller CIEs extending into the early Ordovician. Our Hg and Os data offer no strong evidence that the CIEs

present in our record could have been driven by (globally) elevated volcanism or continental weathering. Organic-carbon and Hg concentrations covary cyclically, providing further evidence of an unperturbed Hg cycle. Mesozoic and Cenozoic CIEs are often linked to enhanced volcanic activity and weathering but similar late Cambrian–Early Ordovician events cannot easily be connected to such external triggers. Our results are more consistent with reduced Early Paleozoic carbon-cycle resilience that allowed small imbalances to develop into large CIEs.

INTRODUCTION

Phanerozoic carbon-isotope excursions (CIEs) are thought to indicate broad-scale carbon-cycle changes. In the geological record, they commonly coincide with biotic radiation and extinction, and are considered critical periods in the evolution of Earth’s environmental systems. The nature of the CIEs changes through time with Paleozoic CIEs generally exceeding the amplitude and length of similar events in the Mesozoic and Cenozoic, a pattern interpreted to reflect gradually increasing carbon-cycle resilience. The increased resilience of the exogenic carbon cycle over the Phanerozoic may result from factors including greater plankton biodiversity, gradual oxygenation of the atmosphere and oceans (Bachan et al., 2017) and, from the Silurian onwards, the proliferation of vascular plants that greatly enhanced the efficiency of continental silicate weathering as a carbon-cycle feedback (Berner, 1998).

Many Mesozoic and Cenozoic CIEs show at least a degree of temporal correlation to emplacement of large igneous provinces (LIPs) (e.g., Ernst et al. 2021), suggesting a causal link. However, erosive and tectonic loss of LIP materials and sedimentary archives (e.g., Park et al., 2021) limits identification of LIP activity coeval with Early Paleozoic CIEs and availability of

proxy data for enhanced volcanism. Hence other mechanisms are often invoked as causing these carbon-cycle perturbations (Reershemius and Planavsky, 2021).

Here we focus on a late Cambrian–Early Ordovician interval that shows substantial carbon-cycle instability. The interval includes the Steptoean Positive Carbon Isotope Excursion (SPICE, 497.5–494.5 million years ago (Ma), the Top of Cambrian isotope Excursion (TOCE, 488 Ma) and the Cambrian-Ordovician boundary spike (COBS, 487 Ma). SPICE, the most significant of these CIEs, was a period of extensive oceanic anoxia and OM burial that is marked globally in marine organic matter (OM) and carbonates by a 2–4‰ positive CIE (e.g., Gill et al., 2011; Saltzman et al., 2011). Coeval fluctuations in sea level and continental weathering have also been proposed (Pulsipher et al., 2021; Yuan et al., 2022) but the trigger for SPICE, and other late Cambrian CIEs, remains elusive.

To study the nature of the late Cambrian–early Ordovician CIEs, we undertook mercury (Hg) and osmium (Os) analyses on sedimentary core samples from the Alum Shale Formation recovered in the Albjära-1 core, southern Sweden (Fig. 1). Previous studies have attributed Hg variability during this period to local changes in oxygenation (Pruss et al., 2019; Hagen et al., 2022) or to elevated volcanism but with their findings limited by low stratigraphic resolution (Bian et al., 2022). Albjära-1 provides a rare, astronomically-tuned long-term (500–484 Ma), near-continuous record without major changes in lithology, depositional environment or oxygenation (Zhao et al., 2022a). The finely (sub-mm) laminated Alum Shale Formation was deposited around 60°S paleolatitude, in a (predominantly) anoxic–euxinic shallow to deep shelf sea that covered most of present-day Scandinavia (Sørensen et al., 2020; Schulz et al., 2021; Zhao et al., 2022a) (Fig. 1). The formation is known for its high concentrations of total organic carbon (TOC; 5–25%), high trace-element concentrations, including U, Mo, V and Zn, and

astronomically modulated sulfur and aluminum (Sørensen et al., 2020; Schulz et al., 2021). Recent studies based on the Alum Shale documented high rhenium (Re), Os and a variable seawater Os-isotope signature (initial $^{187}\text{Os}/^{188}\text{Os}$, hereafter Os_i) (Rooney et al., 2022) during the SPICE interval and high Hg in the upper Cambrian (Bian et al., 2022), which may hint at variations in weathering and volcanism.

Mercury and Os are proxies that, when paired, can be used to assess large-scale subaerial and submarine volcanic activity and continental weathering (Grasby et al., 2019; Dickson et al., 2021). As long as depositional conditions remain relatively stable, elevated Hg loading might be assumed to trace increased igneous activity from LIPs, with subaerial LIPs yielding geographically wider spread sedimentary signals (Grasby et al., 2019; Percival et al., 2021). Mass-dependent and mass-independent fractionation (MDF and MIF) of Hg isotopes may provide insight into depositional pathways of Hg and major source-shifts of Hg in deep-time sediments (Bergquist and Blum, 2007; Bergquist, 2017). Seawater Os isotopes trace the proportion of unradiogenic (mantle- and cosmogenically derived), Os *versus* that of radiogenic Os from continental weathering (e.g., Peucker-Ehrenbrink and Ravizza, 2000). Basalt–seawater interaction releases Os during submarine LIP activity, which can imprint a mantle-like Os-isotope signature on global sea water (Sullivan et al., 2020; Dickson et al., 2021). We present high-resolution sedimentary Hg and Re-Os data for the late Cambrian to investigate whether changes in weathering or volcanism relate to SPICE or other CIEs.

MATERIALS

We analyzed samples from Albjära-1, a ~237-meter fully cored borehole near Svalöv, Sweden (55.935842 N, 13.178478 E) (Fig. 1). A detailed bio- and chemostratigraphy was paired

with radiometric data to anchor astronomically tuned ages for the Alum Shale Formation (215–135 meter core depth (mcd)) and shows that this interval spans 16-Myr of late Cambrian–early Ordovician time (*ca.* 500–484 Ma) (Zhao et al., 2022a; 2022b, Fig. 2). Sedimentary Hg data were acquired from powdered samples used by Zhao et al. (2022a) ($n = 133$) and from additional high-resolution samples across the SPICE interval ($n = 430$, 205–190 mcd, ~5–10 kyr resolution), for which orbital frequencies were examined. New TOC data were generated for the high-resolution samples spanning the SPICE interval ($n = 145$) and combined with existing data (Zhao et al., 2022a). A subset of 22 samples (210–180 mcd, 499–492 Ma) was selected for Re-Os analyses and 12 samples spanning the SPICE interval were analyzed for Hg isotopes. The Supplementary information¹ contains a detailed description of analytical methods.

RESULTS & DISCUSSION

Upper Cambrian–Lower Ordovician mercury

The Alum Shale yields high average Hg (290 ppb) and high TOC (average 8.5% by weight; Fig. 2B, Fig. S2A). Mercury and TOC are positively correlated ($R^2 \sim 0.6$ (SPICE data), ~ 0.5 (SPICE excluding limestone bands), ~ 0.3 (for the entire record)) and Hg/TOC averages around 35 ppb/% (Fig. 2C). The Hg and Hg/TOC values overlap with those obtained from Phanerozoic global organic-rich (>5%) shales (22–650 ppb and 2.3–76.7 ppb/%, 2.5–97.5% quantiles, Grasby et al., 2019). The highest Hg and Hg/TOC (up to 800 ppb, 70 ppb/%) are found in the TOCE interval (~488 Ma). A few ($n = 9$) Hg values in this interval were identified as anomalous by Hg-TOC robust regression (Fig. 2B, Fig. S3) but these are not matched in the nearby Ottenby-2 core (Bian et al., 2022, Fig. S5). Mercury mass accumulation rate (Hg-MAR) varies between 0.1 and 0.3 $\mu\text{g}/\text{m}^2/\text{yr}$, in parallel with TOC-MAR (30–60 $\text{mg}/\text{m}^2/\text{yr}$) (Fig. 2D).

For the broader SPICE interval (498.2–494.2 Ma), appreciable cyclic variability in Hg is observed in the short eccentricity band (~100 kyr) (Fig. 3). The mass-dependent ($\delta^{202}\text{Hg}$ average $-1.14 \pm 0.14\%$ 1 standard deviation) and subtle positive MIF ($\Delta^{199}\text{Hg}$ average $+0.08 \pm 0.03\%$, $\Delta^{200}\text{Hg}$ $+0.03 \pm 0.01\%$) suggest an atmospheric pathway for deposition followed by probably ~complete marine OM Hg scavenging (Blum et al., 2014; Percival et al., 2021).

Anomalous enrichment (>2-fold background) of sedimentary Hg, relative to common carrier phases such as TOC and S, has been linked to enhanced LIP activity (Grasby et al., 2019). Although Hg content for the Alum Shale may appear relatively high, Hg-MAR remains low and Hg/TOC enrichments >2-fold background are rare. A dominant atmospheric depositional pathway for Hg, as suggested by Hg-isotope signatures, is consistent with the very low accumulation (mm/kyr) of (siliciclastic) material in this outer-shelf setting (Zhao et al., 2022b), absence of vascular plants and consequent lack of substantial terrestrial Hg reservoirs that otherwise might have imposed negative MIF and more negative MDF (Yuan et al., 2023).

The Hg-MAR values for the Alum Shale are close to, but slightly lower than, estimated Holocene (non-polluted) atmospheric fluxes ($0.4\text{--}0.6\text{ }\mu\text{g}/\text{m}^2/\text{yr}$; Bindler, 2003). The combination of such low Hg-MAR in the presence of abundant scavenging ligands (OM) and Hg-isotope signature suggests Hg supply could have been limited to atmospheric deposition. The predominantly anoxic–euxinic bottom water conditions during deposition of the Alum Shale and associated SPICE interval may have locally reduced Hg-MAR (Frieling et al., 2023). Mercury loss during maturation may also have reduced apparent Hg-MAR (Liu et al., 2022) but this would likely have been a minor factor as Hg is effectively immobile below 250 °C in clay-rich lithologies (Chen et al. 2022).

In a Hg supply-limited system, cyclic changes in the siliciclastic flux (Al), as shown by Zhao et al. (2022b), may variably dilute a steady TOC and Hg supply. Indeed, as with Al, cyclicity in Hg is focused around the (short) eccentricity and obliquity frequency (Fig. 3) suggesting orbital changes in siliciclastics have modulated Hg content. The low Hg-MAR, cyclic modulation of Hg in parallel with TOC, and Hg-isotope signatures, all indicate a late Cambrian Hg cycle unperturbed by extensive volcanic Hg fluxes.

Enhanced mantle-derived Os input, basin restriction or diminished Os inventory?

The older part of the Re-Os record (499–495.5 Ma) is marked by gradually declining Re (average ~16 ppb) and ^{192}Os (~0.2 ppb) contents with a nadir between 497.5–495.5 Ma (Fig. 2F,G). After 495 Ma values reach up to 165 ppb Re and 2 ppb ^{192}Os , following which Re and ^{192}Os return to pre-SPICE background levels (Fig. 2F). Age-corrected initial $^{187}\text{Os}/^{188}\text{Os}$ (Os_i) hover around ~0.8 for the entire 7-Myr period. Os_i decreases from ~0.8 to 0.4–0.6 from 498–496 Ma, and deeper minima (Os_i ~0.2 and 0.4) are present between 495 and 493 Ma, the lower of which approaches the unradiogenic end-member (~0.13) (cf. Peucker-Ehrenbrink and Ravizza, 2000) (Fig. 2G).

A study on the nearby Andrarum-3 core (Rooney et al., 2022) showed Os_i variability during SPICE. Albjära-1 and Andrarum-3 show very similar Re and Os contents and Os_i profiles (Fig. S5), but our record extends into older and younger strata. The upper Cambrian Os_i values hover around 0.7–0.8, in line with the initial $^{187}\text{Os}/^{188}\text{Os}$ obtained from a ^{187}Re - ^{188}Os evolution plot of our data (0.71 ± 0.10 ; Fig. S1) and the isochron value of 0.82 ± 0.01 (Rooney et al., 2022). Not all Os_i variability can be linked to changes in mantle and continental weathering fluxes. For example, Os_i for (semi-)restricted basins can differ from the oceanic Os_i signature (Dickson et

al., 2021; 2022) and enhanced drawdown of Os can substantially reduce the whole ocean Os inventory in a similar way to Mo and other trace elements that experience enhanced burial with deoxygenation (Algeo, 2004). The connection to the Iapetus Ocean (Fig. 1) and U-Mo behavior (Zhao et al., 2023) indicate a limited degree of watermass restriction so that Os_i here likely reflects global seawater Os_i . A well-documented drop in Mo accompanies SPICE (Fig. 2E, Gill et al., 2011; Zhao et al., 2022b), interpreted to reflect global Mo drawdown as a result of widespread euxinia (Gill et al., 2011; Zhao et al., 2023). Like Mo, the ^{192}Os content gradually declines through the SPICE interval, which may have resulted in heightened sensitivity in the whole-ocean Os (Fig. 2F). This possibility is particularly relevant because periods with Os_i trends that may be interpreted as elevated mantle input or continental weathering occur during the rising limb of SPICE (498–495.5 Ma) (Fig. 2F, G; and Rooney et al., 2022). For the intervals >495.5 Ma, where ^{192}Os is slowly decreasing, small changes in mantle input and continental weathering may have been amplified by heightened Os_i -sensitivity (Fig. 2F, G). In addition, weathering of young volcanic terranes in equatorial latitudes such as the Kalkarindji LIP (*ca.* 510 Ma) (Park et al., 2021), may have supplied more unradiogenic Os_i (Peucker-Ehrenbrink and Ravizza, 2000). Fluctuations towards unradiogenic Os_i values that occur during the rising limb of SPICE therefore neither provide evidence for nor exclude changes in continental weathering and are not in conflict with previous suggestions of fluctuations in weathering based on Os- and Zn-isotope data (Rooney et al., 2022; Yuan et al., 2022).

Unlike the earlier Os_i excursions, the more unradiogenic Os_i values around 494 Ma coincide with a rise in ^{192}Os , suggesting that heightened Os_i sensitivity did not play a role here. This behavior closely resembles that of Mesozoic Oceanic Anoxic Events associated with submarine LIP volcanism, where fresh basaltic material, strongly enriched in unradiogenic Os,

can interact directly with seawater (e.g., Sullivan et al., 2020). However, in contrast to such signals recorded in Mesozoic sediments, higher Os and more unradiogenic Os_i at the end of SPICE do not seem to be associated with any global exogenic $\delta^{13}\text{C}$ or carbon-cycle changes (Saltzman et al., 2011; Zhao et al., 2022b).

CONCLUSIONS

We employed Hg and Os concentrations and isotopes to resolve the impact of enhanced volcanic activity and weathering on the SPICE (497.5–494.5 Ma) event and other late Cambrian–Early Ordovician (500–486 Ma) CIEs. Mercury varies cyclically with TOC and normalized Hg was stable throughout SPICE and most of the late Cambrian–Early Ordovician. Mercury isotopes indicate Hg was predominantly supplied via atmospheric deposition and, even though a small number of elevated Hg samples appear around TOCE (~ 488 Ma), Hg-MAR remains low throughout the entire 16-Myr-long record, pointing to an unperturbed Hg cycle.

No clear trends in Os_i occur during SPICE and several drops towards unradiogenic values during the event may reflect subtle changes in mantle or weathering fluxes amplified by elevated sensitivity of the global Os reservoir due to drawdown. Elevated Os and a mantle-like Os_i occur towards the top of the SPICE interval (~495 Ma) but there appears to be no relationship with $\delta^{13}\text{C}$ trends. We cannot exclude the possibility that subtle changes in weathering occurred during the rising limb of SPICE but surmise that enhanced volcanic activity, if it occurred during the late Cambrian–early Ordovician, had little overall impact on the carbon cycle. Our data support the view that the high-amplitude CIEs that occurred throughout the Early Paleozoic may not have required external triggers and instead resulted from small instabilities and weak carbon cycle feedbacks (e.g. inefficient silicate weathering) that characterized the nascent carbon cycle.

205

206 **ACKNOWLEDGMENTS**

207 We thank S. Wyatt (Oxford) and A. Bashforth (Natural History Museum, Denmark) for
208 assistance, the Carlsberg Foundation (CF16-0876) and the ERC (Consolidator Grant V-ECHO:
209 ERC-2018-COG-818717-V-ECHO) for funding & 2 reviewers for constructive feedback.

210

211 **REFERENCES**

- 212 Algeo, T.J., 2004, Can marine anoxic events draw down the trace element inventory of seawater?
213 *Geology*, v. 32, no. 12, p. 1057–1060, doi: 10.1130/G20896.1.
- 214 Bachan, A., Lau, K. V., Saltzman, M.R., Thomas, E., Kump, L.R., and Payne, J.L., 2017, A
215 model for the decrease in amplitude of carbon isotope excursions across the Phanerozoic:
216 *American Journal of Science*, v. 317, no. 6, p. 641–676, doi: 10.2475/06.2017.01.
- 217 Bergquist, B.A., 2017, Mercury, volcanism, and mass extinctions: *Proceedings of the National*
218 *Academy of Sciences of the United States of America*, v. 114, no. 33, p. 8675–8677, doi:
219 10.1073/pnas.1709070114.
- 220 Bergquist, B.A., and Blum, J.D., 2007, Mass-dependent and -independent fractionation of Hg
221 isotopes by photoreduction in aquatic systems: *Science*, v. 318, no. 5849, p. 417–420, doi:
222 10.1126/science.1148050.
- 223 Berner, R.A., 1998, The carbon cycle and carbon dioxide over Phanerozoic time: the role of land
224 plants (D. J. Beerling, W. G. Chaloner, & F. I. Woodward, Eds.): *Philosophical*
225 *Transactions of the Royal Society of London. Series B: Biological Sciences*, v. 353, no.
226 1365, p. 75–82, doi: 10.1098/rstb.1998.0192.
- 227 Bian, L., Chappaz, A., Schovsbo, N.H., Nielsen, A.T., and Sanei, H., 2022, High mercury

228 enrichments in sediments from the Baltic continent across the late Cambrian: Controls and
229 implications: *Chemical Geology*, v. 599, 120846, doi: 10.1016/j.chemgeo.2022.120846.

230 Bindler, R., 2003, Estimating the natural background atmospheric deposition rate of mercury
231 utilizing ombrotrophic bogs in Southern Sweden: *Environmental Science and Technology*,
232 v. 37, no. 1, p. 40–46, doi: 10.1021/es020065x.

233 Blum, J.D., Sherman, L.S., and Johnson, M.W., 2014, Mercury isotopes in earth and
234 environmental sciences: *Annual Review of Earth and Planetary Sciences*, v. 42, p. 249–269,
235 doi: 10.1146/annurev-earth-050212-124107.

236 Chen, D., Ren, D., Deng, C., Tian, Z., and Yin, R., 2022, Mercury loss and isotope fractionation
237 during high-pressure and high-temperature processing of sediments: Implication for the
238 behaviors of mercury during metamorphism: *Geochimica et Cosmochimica Acta*, v. 334, p.
239 231–240, doi: 10.1016/j.gca.2022.08.010.

240 Dickson, A.J., Cohen, A.S., and Davies, M., 2021, The Osmium Isotope Signature of
241 Phanerozoic Large Igneous Provinces, *in* Ernst, R.E., Dickson, A.J., and Bekker, A. eds.,
242 Large Igneous Provinces: A Driver of Global Environmental and Biotic Changes, p. 229–
243 246.

244 Dickson, A.J., Davies, M., Bagard, M.-L., and Cohen, A.S., 2022, Quantifying seawater
245 exchange rates in the Eocene Arctic Basin using osmium isotopes: *Geochemical*
246 *Perspectives Letters*, v. 24, p. 7–11, doi: 10.7185/geochemlet.2239.

247 Frieling, J., Mather, T.A., März, C., Jenkyns, H.C., Hennekam, R., Reichart, G.-J., Slomp, C.P.,
248 and van Helmond, N.A.G.M., 2023, Effects of redox variability and early diagenesis on
249 marine sedimentary Hg records: *Geochimica et Cosmochimica Acta*, v. 351, p. 78–95, doi:
250 10.1016/j.gca.2023.04.015.

251 Gill, B.C., Lyons, T.W., Young, S.A., Kump, L.R., Knoll, A.H., and Saltzman, M.R., 2011,
 252 Geochemical evidence for widespread euxinia in the Later Cambrian ocean: *Nature*, v. 469,
 253 no. 7328, p. 80–83, doi: 10.1038/nature09700.

254 Grasby, S.E., Them, T.R., Chen, Z., Yin, R., and Ardakani, O.H., 2019, Mercury as a proxy for
 255 volcanic emissions in the geologic record: *Earth-Science Reviews*, v. 196, 102880, doi:
 256 10.1016/j.earscirev.2019.102880.

257 Hagen, A.P.I., Jones, D.S., Tosca, N.J., Fike, D.A., and Pruss, S.B., 2022, Sedimentary mercury
 258 as a proxy for redox oscillations during the Cambrian SPICE event in western
 259 Newfoundland: *Canadian Journal of Earth Sciences*, v. 59, no. 8, p. 504–520, doi:
 260 10.1139/cjes-2021-0108.

261 Park, Y., Swanson-Hysell, N.L., Lisiecki, L.E., and Macdonald, F.A., 2021, Evaluating the
 262 Relationship Between the Area and Latitude of Large Igneous Provinces and Earth’s Long-
 263 Term Climate State, *in* Ernst, R.E., Dickson, A.J., and Bekker, A. eds., *Large Igneous*
 264 *Provinces: A Driver of Global Environmental and Biotic Changes*, p. 153–168.

265 Percival, L.M.E., Bergquist, B.A., Mather, T.A., and Sanei, H., 2021, Sedimentary Mercury
 266 Enrichments as a Tracer of Large Igneous Province Volcanism, *in* Ernst, R.E., Dickson,
 267 A.J., and Bekker, A. eds., *Large Igneous Provinces: A Driver of Global Environmental and*
 268 *Biotic Changes*, *Geophysical Monograph Series*, American Geophysical Union, p. 247–262.

269 Peucker-Ehrenbrink, B., and Ravizza, G., 2000, The marine osmium isotope record: *Terra Nova*,
 270 v. 12, no. 5, p. 205–219, doi: 10.1046/j.1365-3121.2000.00295.x.

271 Pruss, S.B., Jones, D.S., Fike, D.A., Tosca, N.J., and Wignall, P.B., 2019, Marine anoxia and
 272 sedimentary mercury enrichments during the Late Cambrian SPICE event in northern
 273 Scotland: *Geology*, v. 47, no. 5, p. 475–478, doi: 10.1130/G45871.1.

274 Pulsipher, M.A., Schiffbauer, J.D., Jeffrey, M.J., Huntley, J.W., Fike, D.A., and Shelton, K.L.,
 275 2021, A meta-analysis of the Steptoean Positive Carbon Isotope Excursion: The SPICEraq
 276 database: *Earth-Science Reviews*, v. 212, 103442, doi: 10.1016/j.earscirev.2020.103442.
 277 Rooney, A.D., Millikin, A.E.G., and Ahlberg, P., 2022, Re-Os geochronology for the Cambrian
 278 SPICE event: Insights into euxinia and enhanced continental weathering from radiogenic
 279 isotopes: *Geology*, v. 50, no. 6, p. 716–720, doi: 10.1130/G49833.1.
 280 Saltzman, M.R., Young, S.A., Kump, L.R., Gill, B.C., Lyons, T.W., and Runnegar, B., 2011,
 281 Pulse of atmospheric oxygen during the late Cambrian: *Proceedings of the National*
 282 *Academy of Sciences of the United States of America*, v. 108, no. 10, p. 3876–3881, doi:
 283 10.1073/pnas.1011836108.
 284 Schulz, H.M., Yang, S., Schovsbo, N.H., Rybacki, E., Ghanizadeh, A., Bernard, S., Mahlstedt,
 285 N., Krüger, M., Amann-Hildebrandt, A., Krooss, B.M., Meier, T., and Reinicke, A., 2021,
 286 The Furongian to Lower Ordovician Alum Shale Formation in conventional and
 287 unconventional petroleum systems in the Baltic Basin – A review: *Earth-Science Reviews*,
 288 v. 218, 103674, doi: 10.1016/j.earscirev.2021.103674.
 289 Sørensen, A.L., Nielsen, A.T., Thibault, N., Zhao, Z., Schovsbo, N.H., and Dahl, T.W., 2020,
 290 Astronomically forced climate change in the late Cambrian: *Earth and Planetary Science*
 291 *Letters*, v. 548, 116475, doi: 10.1016/j.epsl.2020.116475.
 292 Sullivan, D.L., Brandon, A.D., Eldrett, J., Bergman, S.C., Wright, S., and Minisini, D., 2020,
 293 High resolution osmium data record three distinct pulses of magmatic activity during
 294 cretaceous Oceanic Anoxic Event 2 (OAE-2): *Geochimica et Cosmochimica Acta*, v. 285,
 295 p. 257–273, doi: 10.1016/j.gca.2020.04.002.
 296 Yuan, C., Liu, S., Chen, J., and Fang, L., 2022, Zinc isotopic evidence for enhanced continental

weathering and organic carbon burial during the late Cambrian SPICE event:
 Palaeogeography, Palaeoclimatology, Palaeoecology, v. 608, 111302, doi:
 10.1016/j.palaeo.2022.111302.

Yuan, W., Liu, M., Chen, D., Xing, Y., Spicer, R.A., Chen, J., Them, T.R., Wang, X., Li, S.,
 Guo, C., Zhang, G., Zhang, L., Zhang, H., and Feng, X., 2023, Mercury isotopes show
 vascular plants had colonized land extensively by the early Silurian: Science Advances, v.
 9, no. 17, eade9510, doi: 10.1126/sciadv.ade9510.

Zhao, Z., Ahlberg, P., Thibault, N., Dahl, T.W., Schovsbo, N.H., and Nielsen, A.T., 2022a,
 High-resolution carbon isotope chemostratigraphy of the middle Cambrian to lowermost
 Ordovician in southern Scandinavia: Implications for global correlation: Global and
 Planetary Change, v. 209, 103751, doi: 10.1016/j.gloplacha.2022.103751.

Zhao, Z., Pang, X., Zou, C., Dickson, A.J., Basu, A., Guo, Z., Pan, S., Nielsen, A.T., Schovsbo,
 N.H., Jing, Z., and Dahl, T.W., 2023, Dynamic oceanic redox conditions across the late
 Cambrian SPICE event constrained by molybdenum and uranium isotopes: Earth and
 Planetary Science Letters, v. 604, 118013, doi: 10.1016/j.epsl.2023.118013.

Zhao, Z., Thibault, N.R., Dahl, T.W., Schovsbo, N.H., Sørensen, A.L., Rasmussen, C.M.Ø., and
 Nielsen, A.T., 2022b, Synchronizing rock clocks in the late Cambrian: Nature
 Communications, v. 13, 1990, doi: 10.1038/s41467-022-29651-4.

FIGURE CAPTIONS

Figure 1. Map of Scandinavia (western Baltica) showing the location of the Albjära-1
 (this study), Ottenby-2 (Bian et al., 2022) and Andrarum-3 (Rooney et al., 2022) cores (redrawn

from Zhao et al., 2022b) with inset showing the late Cambrian position of Baltica (redrawn from Yuan et al., 2022).

Figure 2. Data for the upper Cambrian (upper Miaolingian and Furongian)–Lower Ordovician Alum Shale of the Albjära-1 core. A. Trilobite biostratigraphy and carbon-isotope ratios ($\delta^{13}\text{C}$) of total organic carbon (TOC) (Zhao et al., 2022a), B. Mercury content, regression outliers marked (*), C. TOC-normalized Hg, D. Mercury and TOC mass accumulation rates (MAR). E. Molybdenum content (Zhao et al., 2022b), 3-cm moving average. F. Sedimentary Re and ^{192}Os content. G. Osmium-isotope ($^{187}\text{Os}/^{188}\text{Os}$) ratio at time of deposition, Os_i . CIE abbreviations: Steptoean Positive Carbon Isotope Excursion (SPICE), Upper and Lower *Peltura scarabaeoides* Spike (U/LPSS), Top of Cambrian Excursion (TOCE), *Acerocarina* positive spike (APS) and Cambrian–Ordovician Boundary Spike (COBS) as recognized in Zhao et al. (2022a).

Figure 3. A. Multi-taper method/auto-regression (MTM/AR) spectral analysis of Al for the high-resolution interval encompassing SPICE (494.2–498.2 Ma). B. As panel A for Hg.

¹Supplemental Material containing a detailed description of analytical methods. Please visit <https://doi.org/10.1130/XXXX> to access the supplemental material, and contact editing@geosociety.org with any questions.

Figure 1

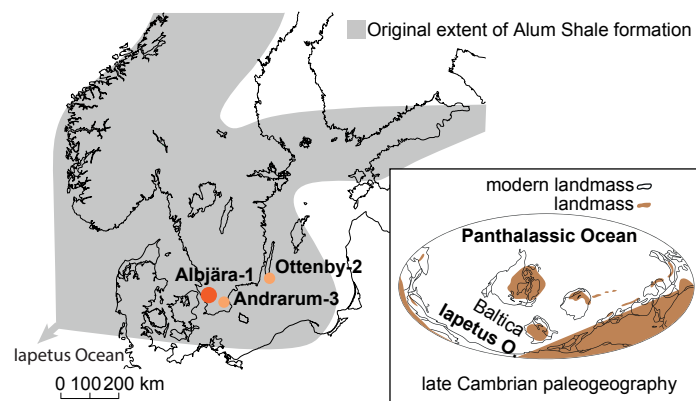
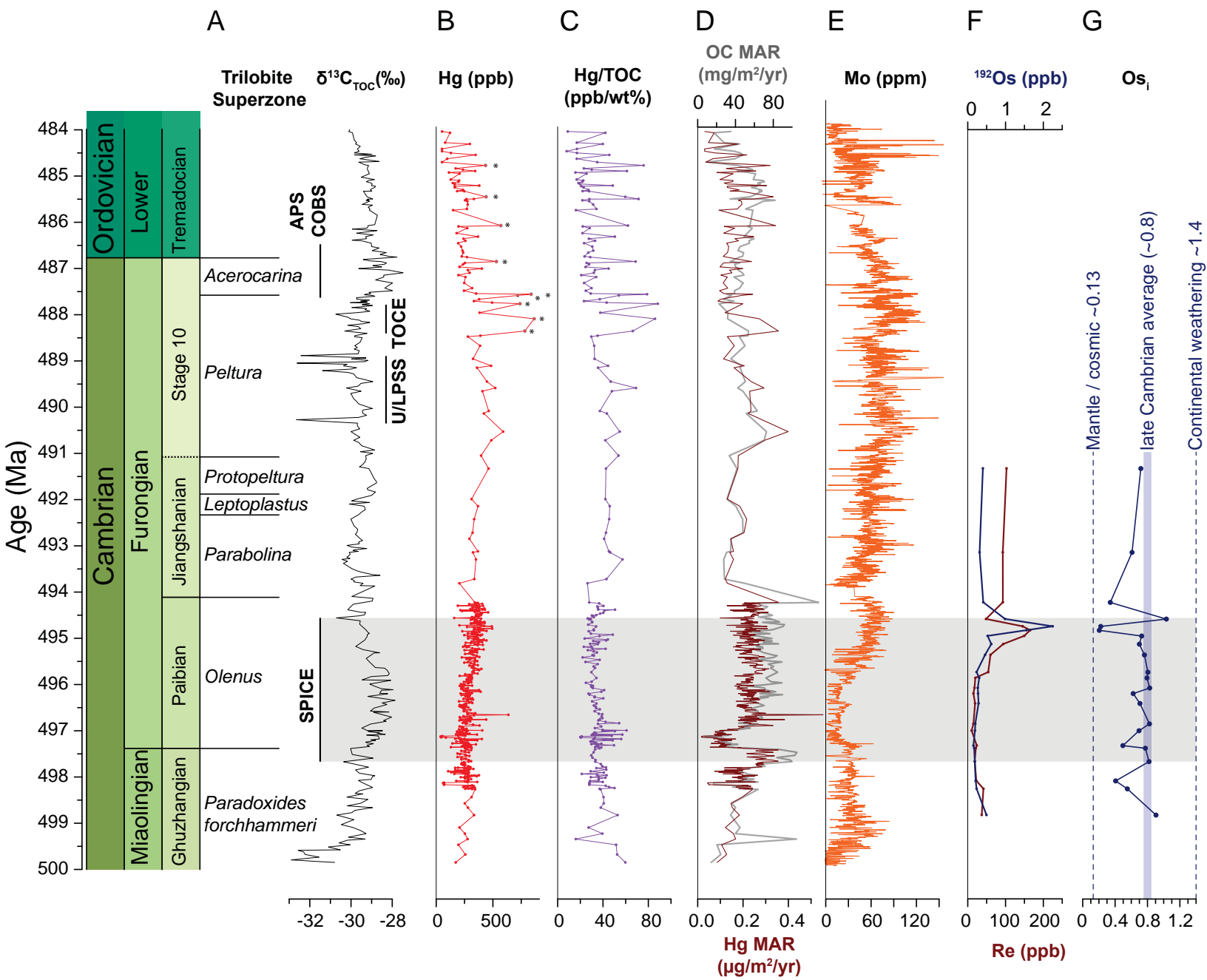
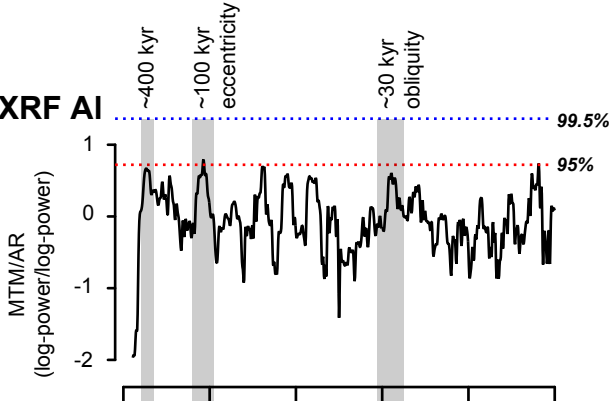


Figure 2



A

XRF AI

B

Hg